ORIGINAL ARTICLE

JBMR®

Targeted Disruption of *Shp2* in Chondrocytes Leads to Metachondromatosis With Multiple Cartilaginous Protrusions

Harry KW Kim,[1,2] Gen-Sheng Feng,[3] Di Chen,[4] Philip D King,[5] and Nobuhiro Kamiya[1,2]

[1]Texas Scottish Rite Hospital for Children, Dallas, TX, USA
[2]Orthopaedic Surgery, University of Texas Southwestern Medical Center, Dallas, TX, USA
[3]Department of Pathology and Division of Biological Sciences, University of California San Diego, La Jolla, CA, USA
[4]Department of Biochemistry, Rush University Medical Center, Chicago, IL, USA
[5]Department of Microbiology and Immunology, University of Michigan Medical School, Ann Arbor, MI, USA

ABSTRACT

Metachondromatosis is a benign bone disease predominantly observed in the hands and feet of children or young adults demonstrating two different manifestations: a cartilage-capped bony outgrowth on the surface of the bone called exostosis and ectopic cartilaginous nodules inside the bone called enchondroma. Recently, it has been reported that loss-of-function mutations of the *SHP2* gene, which encodes the SHP2 protein tyrosine phosphatase, are associated with metachondromatosis. The purpose of this study was to investigate the role of SHP2 in postnatal cartilage development, which is largely unknown. We disrupted *Shp2* during the postnatal stage of mouse development in a chondrocyte-specific manner using a tamoxifen-inducible system. We found tumor-like nodules on the hands and feet within a month after the initial induction. The SHP2-deficient mice demonstrated an exostosis-like and enchondroma-like phenotype in multiple bones of the hands, feet, and ribs as assessed by X-ray and micro-computed tomography (CT). Histological assessment revealed the disorganization of the growth plate cartilage, a cartilaginous protrusion from the epiphyseal bone, and ectopic cartilage nodules within the bones, which is consistent with the pathological features of metachondromatosis in humans (ie, both exostosis and enchondroma). At molecular levels, we observed an abundant expression of Indian hedgehog protein (IHH) and fibroblast growth factor 2 (FGF2) and impaired expression of mitogen-activated protein kinases (MAPK) in the affected cartilage nodules in the SHP2-deficient mice. In summary, we have generated a mouse model of metachondromatosis that includes manifestations of exostosis and enchondroma. This study provides a novel model for the investigation of the pathophysiology of the disease and advances the understanding of metachondromatosis. This model will be useful to identify molecular mechanisms for the disease cause and progression as well as to develop new therapeutic strategies in the future. © 2014 American Society for Bone and Mineral Research.

KEY WORDS: EXOSTOSIS; ENCHONDROMA; CARTILAGE-SPECIFIC KNOCK-OUT MOUSE; SHP2; METACHONDROMATOSIS

Introduction

Metachondromatosis (MC, OMIM 156250) is a disorder found primarily in children or young adults that affects bone growth, where benign bone tumors produce lumps, mostly on the hands and feet. The condition has an autosomal dominant pattern of inheritance and is characterized by exostoses (ie, a benign bony growth projecting outward from a bone surface) that commonly affect the bones of the hands and feet (ie, phalanges and metacarpals/metatarsals) and enchondroma of the metaphysis of the long bones and the iliac crest.[1,2] Multiple exostoses of the classic type known as multiple hereditary exostosis (MHE, OMIM 133700)[3] is clinically distinct from metachondromatosis because involvement of the hands and feet is the rule in metachondromatosis but is unusual in classic multiple exostoses.[4] In addition, MHE patients do not develop enchondroma. However, the difference in disease mechanisms between metachondromatosis and classic multiple exostoses is unclear. Recently, human genetic studies using whole genome sequencing and linkage analysis revealed an association between germline inactivating mutations of SHP2 with metachondromatosis.[1,2]

Src homology-2 (SHP2)-containing protein tyrosine phosphate, also known as protein-tyrosine phosphatases nonreceptor type 11 (PTPN11), plays a central role in RAS/mitogen-activated protein kinase (MAPK) signaling downstream of several receptor tyrosine kinases including the epidermal growth factor receptor (EGFR) and fibroblast growth factor receptor (FGFR).[5,6] In

Received in original form April 16, 2013; revised form June 27, 2013; accepted July 19, 2013. Accepted manuscript online August 8, 2014.
Address correspondence to: Nobuhiro Kamiya, MD, PhD, Texas Scottish Rite Hospital for Children, 2222 Welborn Street, Dallas, TX 75219, USA.
E-mail: Nobby.Kamiya@tsrh.org
Additional Supporting Information may be found in the online version of this article.
Journal of Bone and Mineral Research, Vol. 29, No. 3, March 2014, pp 761–769
DOI: 10.1002/jbmr.2062
© 2014 American Society for Bone and Mineral Research

general, SHP2 promotes RAS/MAPK signal transduction downstream of growth factor receptors.[6,7] SHP2 is ubiquitously expressed in the brain in particular[8] and is involved in the differentiation of multiple cell types and in body organization.[9] Homozygous SHP2$^{-/-}$ mice are embryonic lethal at mid-gestation as a result of multiple defects in gastrulation and mesodermal patterning.[10] The role of SHP2 in skeletal development, however, is largely unknown. In our previous work, we ablated the *Shp2* gene postnatally in all somatic cells of the body and found multiple skeletal abnormalities including scoliosis, kyphosis, osteopetrosis, and growth plate disturbance with cartilage abnormalities.[11] Given growth plate disturbances in these induced SHP2-deficient mice, we postulated that it would be important to specifically investigate the role of SHP2 in chondrocytes during postnatal cartilage development and remodeling.

Although mutations in *SHP2* are known to be causative of metachondromatosis, the pathophysiology of metachondromatosis related to the onset and the progression of exostoses in hands and feet is still unknown. Further progress in understanding the mechanisms of metachondromatosis is limited by the availability of human subjects. To understand the pathophysiology of the disease and to develop new therapeutic strategies, an animal model for metachondromatosis is much needed. The purpose of this study was to investigate the role of SHP2 in chondrocytes. For this purpose, we generated inducible chondrocyte-specific SHP2-deficient mice. Loss of SHP2 in chondrocytes during the postnatal mouse stage resulted in the development of metachondromatosis. This mouse model will be useful to understand the mechanism of this disease and possible means of intervention in pediatric and young adult patients.

Materials and Methods

Generation of chondrocyte-specific SHP2-deficient mice

To delete the *Shp2* gene specifically in chondrocytes, we used a transgenic mouse line expressing Cre recombinase under the control of the type II collagen promoter (ie, *Col2a1CreERt2* mice), which is inducible by tamoxifen administration.[12] We bred the *Col2a1-CreERt2* mice with *Shp2* floxed (*Shp2fx/fx*) mice to generate experimental *Col2a1CreERt2:Shp2fx/fx* mice and control *Shp2fx/fx* mice. To induce a gene disruption in vivo, we injected tamoxifen intraperitoneally into mice at a concentration of 1 mg per mouse per injection, as described in previously.[12] Tamoxifen was administered twice weekly for 5 weeks (ie, a total of 10 injections) to both the experimental and the control animals from 4 weeks after birth. ROSA-lacZ reporter mice (*Gt(ROSA)26Sor^{tm1Sor}*) were used to check Cre activity using the same tamoxifen administration regimen.[13]

Genotyping

To confirm the genotypes of the mice, a small piece of ear was digested with 50 mM KOH at 95°C for 1 hour followed by the addition of 1 M Tris-HCl. The polymerase chain reaction (PCR) was carried out using REDTaq (Sigma-Aldrich, St. Louis, MO, USA) and 0.2 mM deoxynucleotide (dNTP) together with the following primers: Col2a1CreERt2 (5′-CGA ACA TCT TCA GGT TCT GCG G and 5′-GTC GAT GCA ACG AGT GAT GAG G, annealing temperature 65°C, expected size 190 base pair) and SHP2 (5′-ACG TCA TGA TCC GCT GTC AG and 5′-ATG GGA GGG ACA GTG CAG TG, annealing temperature 51°C, expected size 400 base pair for floxed allele and 300 base pair for wild-type allele).

RNA isolation and real-time RT-PCR

Total RNA was isolated from the rib cartilage of three independent mice per group using an RNA isolation kit (Qiagen, Germantown, MD, USA). cDNA was synthesized using the SuperScript Preamplification System (Invitrogen, Carlsbad, CA, USA). PCR reactions, data quantification, and analysis were performed according to the manufacturer's standard protocol of the TaqMan gene expression assay using the ABI PRISM 7500 sequence detection system (Applied Biosystems, Rotkreuz, Switzerland). The reaction volume was 20 μL/well in 96-well plates. SHP2 (Hs00275784_m1) and control glyceraldehyde-3-phosphate dehydrogenase (GAPDH) (Hs99999905_m1) primer/probe sets were predesigned (Applied Biosystems). All measurements were performed in triplicate and analyzed using the $2^{-\Delta\Delta C(t)}$ method.[14]

Gross morphology, radiography, and micro-computed tomography (CT) analysis

For gross morphology, photographs of the hands and feet were taken immediately after the mice were euthanized. Radiographic images of the hands, feet, ribs, and forearms were obtained using a Faxitron X-ray system (Faxitron, Tucson, AZ, USA). For a micro-CT scan (SkyScan 1172 Micro-CT, Bruker MicroCT, Kontich, Belgium), each undecalcified specimen was wrapped with gauze soaked in 70% ethanol and scanned with a 50 kV and 200 μA setting and a 0.5-mm aluminum filter. The resolution was set to 26.6 microns per pixel, and each rotation step was 0.70 degrees over a range of 180 degrees. After reconstruction with NRecon Reconstruction software (version 1.6.8.), all serial section grayscale images were set to a threshold to identify the bone that matched the original grayscale X-ray and to remove any soft-tissue contribution. The binarized three-dimensional images were visualized with CTVox (version 2.4).

Histology and immunostaining

Immediately after euthanization, bones were harvested and fixed with 10% formalin for 5 days followed by decalcification with 10% EDTA for 5 days. Bones were embedded in paraffin, and 3-μm sections were prepared. Hematoxylin and eosin (H&E) staining was performed following a standard protocol as previously described.[15,16] For the detection of the cartilage matrix (ie, chondroitin sulfate), Safranin O staining with Fast Green counter-staining was performed.

For β-galactosidase (β-gal) staining on whole tissues, bones (ie, hands and feet) were fixed in 4% paraformaldehyde and stained with X-gal as described previously.[15,17]

For immunostaining, bones (ie, hands, feet, forearms, ribs) were rinsed with PBS and fixed with 4% paraformaldehyde for 20 minutes. Bones were embedded in paraffin, and 3-μm sections were prepared. Immunostaining was performed using rabbit polyclonal antibodies against Indian hedgehog (1:1000, Abcam, Cambridge, MA, USA), phospho-Erk (1:50, Cell Signaling Technology, Danvers, MA, USA), FGF2 (1:400, Abcam) and SHP2 (1:200, BioVision, Milpitas, CA, USA), followed by secondary antibodies. Antibody binding was visualized with 3, 3′-diaminobenzidine tetrahydrochloride (DAB) before a brief counter-staining with hematoxylin (Invitrogen). Negative controls without primary antibodies were used.

Statistical analysis

Experiments were performed using three to five mice per group. Each assay was performed in triplicate. Data were expressed as mean ± SE. All statistical analyses were performed using a one-sample two-tailed Student's *t* test. Any *p* values <0.05 were considered statistically significant.

Results

Generation of SHP2 cKO mice

To demonstrate that in *Col2a1CreERt2Cre* transgenic mice Cre activity is limited to chondrocytes, we generated *Col2a1-CreERt2 Gt(ROSA)26Sor*^{tm1Sor} lacZ reporter mice. Mice were injected twice weekly with tamoxifen for 5 weeks starting at 4 weeks of age, after which bone preparations were stained with X-gal to reveal sites of Cre activity (Fig. 1*A*). Cre activity was detectable only in cartilage of growth plates, thus confirming targeting of Cre to this cell type. To delete SHP-2 in chondrocytes, we next generated *Col2a1CreERt2:Shp2fx/fx* mice. After genotypic identification of experimental *Col2a1-CreERt2:Shp2fx/fx* mice and control *Shp2fx/fx* mice (Fig. 1*B*), tamoxifen was injected into both groups using the same regimen (ie, initiated in 4-week-old mice). Rib cartilage was then harvested from mice, and expression of *Shp2* RNA was determined by quantitative RT-PCR. The expression of *Shp2* was significantly reduced in the cartilage of the *Col2a1CreERt2: Shp2fx/fx* mice compared with the controls (Fig. 1*C*). Similarly, SHP2 protein levels were reduced in *Col2a1CreERt2:Shp2fx/fx* rib cartilage compared with the control rib cartilage as assessed by immunostaining (Fig. 1*D*). Hereafter, tamoxifen-treated *Col2a1CreERt2:Shp2fx/fx* and *Shp2fx/fx* mice are referred to as SHP-2 cartilage-specific knockout mice (SHP2 cKO) and controls, respectively.

The gross morphology of the hands and feet of SHP2 cKO mice

Two weeks after tamoxifen was first administered to the mice, visible nodule formations in the dorsal hands of the SHP2 cKO mice were observed. These nodules developed and grew under the skin over time until euthanization of mice at 12 weeks of age (Fig. 2*A*). The nodules on the dorsal hands were palpable and whitish without redness and appeared to be attached to the bony tissues of the hands when the skin was removed (Fig. 2*B*). Similarly, we observed multiple nodules in the dorsal feet of the SHP2 cKO mice (Fig. 2*C*). The nodules on hands and feet were preferentially located on the dorsal side rather than the ventral side. We also observed nodules in the wrist and ankle joints (Fig. 2*C*). Notably, no nodules or skeletal abnormalities were observed in heterozygous SHP2-deficient mice (*Col2a1CreERt2: Shp2fx/+*, data not shown). In addition, there was no difference between sexes in the severity of the lesion.

Radiographic and micro-CT assessments of the hands and feet of SHP2 cKO mice

Because the nodules appeared to be connected to the bony tissue, we performed X-rays using undecalcified samples. We identified multiple nodules in the SHP2 cKO hands with comparable radiodensity to the native hand bones (Fig. 2*D*). The nodules were found close to multiple hand joints including the metacarpal-phalangeal and the proximal interphalangeal joints. In particular, distal metacarpal bones were consistently affected in the SHP2 cKO hands. The severity of nodule formation varied among the SHP2 cKO mice at the endpoint (ie, 12 weeks). Similarly, we identified multiple nodules in the SHP2 cKO feet with similar radiodensity to the native foot bones (Fig. 2*E*). Generally, the hand phenotype was more severe than the foot phenotype in the SHP2 cKO mice.

We also examined the three-dimensional (3D) structure of the hands and feet using undecalcified specimens by micro-CT and analyzed the location of bony or calcified/mineralized nodules in relation to the native bone in the SHP2 cKO mice. Micro-CT 3D images of the hands showed multiple nodules between digits (ie, metacarpals, phalanges) and around joints (ie, metacarpal-phalangeal and proximal-interphalangeal joints) (Fig. 3*A*). The ectopic nodules appeared structurally different from the endogenous hand digits. Similarly, micro-CT 3D images of the foot showed multiple nodules around the joints (ie, metatarsal-phalangeal and ankle joints) (Fig. 3*B*). In addition, we identified bony nodules arising from the metaphyseal region of the metacarpal bone as assessed by sequential frontal micro-CT images (Fig. 3*C*).

Histological assessment of the hands of SHP2 cKO mice

H&E staining revealed that the nodules were consistently located around the metacarpal-phalangeal joints in the SHP2 cKO hands (Fig. 4*A, B*). Interestingly, the nodule was predominantly covered by a fibrous cap (Fig. 4*B*). The nodules arose from the metaphyseal region of the distal metacarpal bone and showed a cartilaginous staining pattern with cells that resembled prehypertrophic or hypertrophic chondrocytes. The cartilaginous matrix in the nodules was characteristically stained red by Safranin O staining, whereas cartilaginous tissue was not present in the distal metaphysis of the control metacarpal bone (Fig. 4*C, D*). Upon closer examination, the nodules were seen to originate from the region between the perichondrium and periosteum that is named the groove of Ranvier (Fig. 4*E, F*). Safranin O staining revealed the cartilaginous matrix in the nodules originated from the groove of Ranvier in the distal metacarpal bone of the SHP2 cKO hands (Fig. 4*G–I*). Note that the early stage of disease development was observed, although the growth plate was already absent at this stage (Fig. 4*F, I*), suggesting that a certain cell population in the periosteum or perichondrium was likely to cause ectopic cartilage formation independent from the presence of growth plate cartilage. Similarly, in the feet, ectopic cartilaginous nodules were formed in the metaphysis of the distal metatarsal bones in the SHP2 cKO mice as assessed by H&E and Safranin O staining (Supplemental Fig. S1).

Exostosis-like phenotype in forearms and ectopic cartilage in ribs of SHP2 cKO mice

We also identified a bone deformity in the distal radius and ulna in the SHP2 cKO mice compared with controls as assessed by X-ray and 3D micro-CT (Fig. 5*A, B*). The deformity was present primarily in the metaphysis of the radius and ulna, and the shape of the distal radius and ulna appeared to be widened in the SHP2 cKO mice compared with the controls. More intriguingly, the pattern of bony protrusion looked similar to the one seen in patients with exostosis.[18,19] H&E staining revealed a cartilaginous component in the bony protrusion of the distal radius and ulna in the SHP2 cKO mice (Fig. 5*D*). Safranin O staining showed an ectopically formed cartilaginous matrix in the distal radius and ulna of the SHP2 cKO mice (Fig. 5*D*).

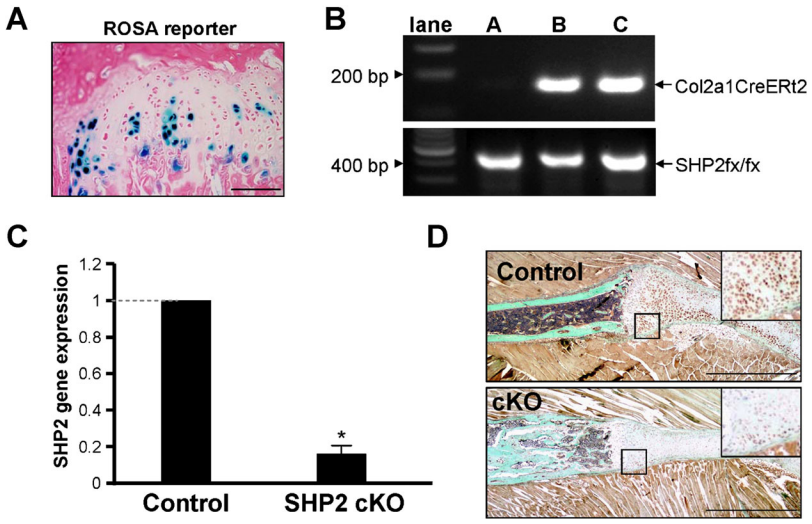

Fig. 1. Generation of SHP2 cKO mice. (*A*) Cre activity in *Col2a1CreERt2:ROSA26-lacz* mice was determined by X-gal staining (blue). Shown is the rib growth plate 5 weeks after administration of tamoxifen to 4-week old-mice. (*B*) Genotype of the SHP2 cKO (*Col2a1CreERt2:Shp2fx/fx)* and control (*Shp2fx/fx* mice) was determined by PCR of mouse ear DNA (lane A, control mouse; lanes B and C, SHP2 cKO mice). (*C*) Relative expression of *Shp2* in rib cartilage from control and SHP2 cKO mice was determined by quantitative RT-PCR 5 weeks after administration of tamoxifen to 4-week-old mice. Amounts of *Shp2* RNA were significantly reduced in the SHP2 cKO mice compared with the controls set as 1.0 ($^*p < 0.01$). (*D*) Rib cartilage from control and SHP2 cKO mice was stained with a SHP2 antibody. SHP2 protein expression was substantially reduced in the SHP2 cKO cartilage compared with the controls.

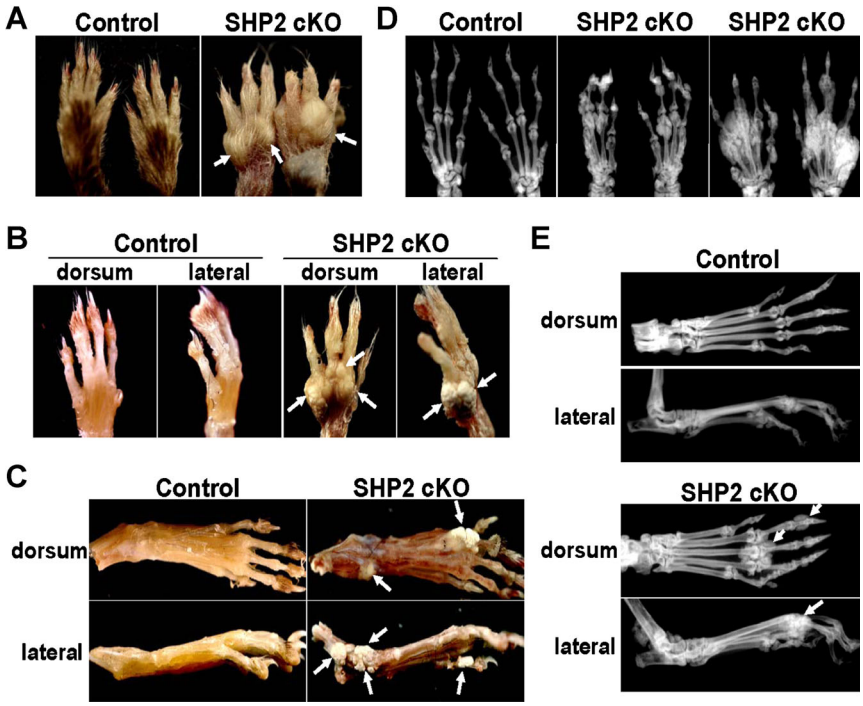

Fig. 2. Gross morphology and radiographic assessment of hands and feet in SHP2 cKO mice. (*A*) Tamoxifen was administered to control and SHP2 cKO mice 4 weeks after birth. Multiple nodules in the hands were detected within 2 to 3 weeks in the SHP2 cKO mice, which progressed and became larger over time. Shown are nodules on the hands of SHP2 cKO mice at 12 weeks of age (arrows). (*B*) Images are of hands of the same mice in (*A*) after skin removal. The nodules in the SHP2 cKO mice were attached to the bony tissue of the hands. (*C*) Images were taken after the skin was removed from the feet. The nodules in the SHP2 cKO mice were attached to the bony tissue of the feet. (*D*) Nodules in the hands of the SHP2 cKO mice at 12 weeks of age were assessed by X-ray. X-ray images showed multiple extra bony masses adjacent to the metacarpal-phalangeal and proximal interphalangeal joints with a similar intensity to the native digits. Some digit bones (ie, metacarpals, phalanges) were deformed around the nodules. Different degrees of progression were observed in SHP2 cKO mice from mild (middle panel) to severe (right panel). (*E*) Nodules in the feet of the SHP2 cKO mice at 12 weeks of age were assessed by X-ray. X-ray images showed an extra bony mass (white arrows) adjacent to the metatarsal-phalangeal joints and distal phalangeal bones with similar intensity to the digits (ie, metatarsals, phalanges).

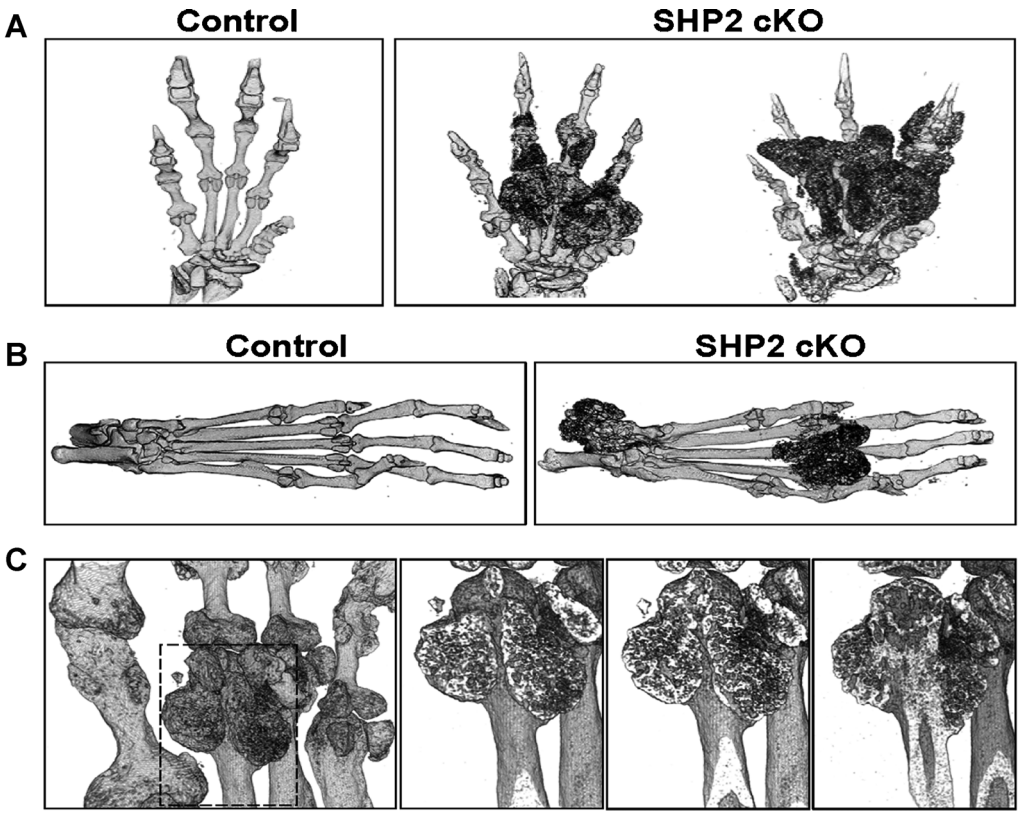

Fig. 3. Micro-CT assessment of hands and feet of SHP2 cKO mice. (*A*) Nodules in the hands of the SHP2 cKO mice at 12 weeks of age were assessed by micro-CT using undecalcified samples. Three-dimensional reconstruction of hand images showed multiple nodules between the digits (metatarsals, phalanges) and around the joints (metacarpal-phalangeal and proximal interphalangeal joints). The severity of phenotype varied in the SHP2 cKO mice. (*B*) Nodules in the feet of the SHP2 cKO mice at 12 weeks of age were assessed by micro-CT using undecalcified samples. Three-dimensional reconstruction of the foot images showed multiple nodules around the joints (metatarsal-phalangeal and ankle joints). (*C*) The extra bony mass in the digits (distal metacarpal bone) was analyzed by micro-CT. The sequential frontal images showed a three-dimensional development of bony mass originating from the distal metaphyseal region of the metacarpal bone. The boxed area in the left image was magnified sequentially in the right three images.

In addition, we also identified heterogeneous radiodensity in the SHP2 cKO rib bones compared with the control rib bones as assessed by X-ray and 3D micro-CT (Fig. 5*C*). H&E staining showed an irregular rib cartilage surface and a disorganized column formation in the rib growth plate cartilage in the SHP2 cKO mice (Fig. 5*E*). Safranin O staining showed a disorganized staining pattern with prominence of hypertrophic chondrocyte clusters at the perichondrium-to-rib cartilage junction (arrows) in the SHP2 cKO rib (Fig. 5*E*). In addition, Safranin O staining showed multiple cartilage islands within the rib trabecular bone of the SHP2 cKO mice (Fig. 5*E*), suggesting an abnormal cartilage remodeling within bone as seen in the patients with enchondroma.

Abundant IHH expression and impaired MAPK signaling in cartilaginous nodules

We further analyzed exostosis-like bone phenotype in the SHP2 cKO hands and feet and enchondroma-like phenotype in the cKO ribs at molecular levels. Cre activity within bone deformities was monitored using ROSA reporter mice and X-gal staining. X-gal staining was noted in the cartilaginous nodules that developed from the metaphysis and in a small population of cells in the perichondrium and periosteum adjacent to the groove of Ranvier (Supplemental Fig. S2). Indian hedgehog protein (IHH) is known to be primarily expressed by prehypertrophic chondrocytes in the growth plate and potentially affects the perichondrium and periosteum around the groove of Ranvier.[20] In SHP2 cKO mice, the expression domain of IHH was elongated in the rib growth plate cartilage compared with the controls (Fig. 6*A*, left and middle panels). Most interestingly, the IHH was abundantly expressed in the ectopic cartilaginous nodules in SHP2 cKO rib bones (Fig. 6*A*, middle panel). Consistently, IHH was expressed in the cartilaginous nodule in hands (Fig. 6*A*, right panel). In the early stage of disease development in hands and ribs, we observed prehypertrophic-like cells that abundantly express IHH in the periosteum (Supplemental Fig. S3). Activation of the MAPK, extracellular-regulated kinases 1 and 2 (Erk1 and 2), was assessed using an anti-phospho-Erk1/2 antibody. In the control mice, activated MAPK were identified in the hypertrophic chondrocytes in the control rib growth plate cartilage (Fig. 6*B*, left panel). However, there was much reduced activated MAPK in hypertrophic chondrocytes in SHP2 cKO cartilage (Fig. 6*B*, middle panel), even in the early stage of disease development (Fig. 6*B*, right panel). Note that the cell size of prehypertrophic and hypertrophic chondrocytes was much larger in SHP2 cKO

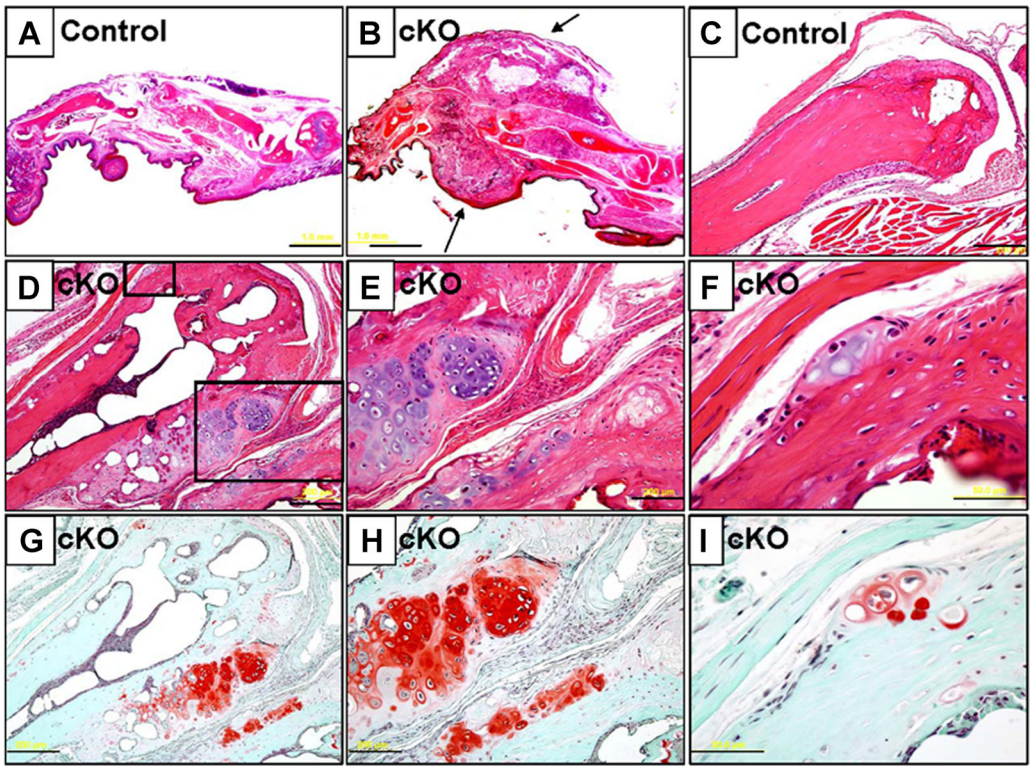

Fig. 4. Histological assessment of hands of SHP2 cKO mice. (*A, B*) H&E-stained sagittal sections of digits from control (*A*) and SHP2 cKO mice (*B*) at 12 weeks of age. Note an extra bony mass covered by a fibrous cap around the metacarpal-phalangeal joint in the SHP2 cKO mice. (*C–F*) H&E-stained sections of distal metacarpal bones of control mice (*C*) and SHP2 cKO mice (*D–F*) at 12 weeks of age. Extra bony nodules were observed in the distal metaphyseal region of the metacarpal bone of the SHP2 cKO mice. The boxed fields (*D*) were magnified (*E, F*). (*G–I*) Serial sections of distal metacarpal bones of SHP2 cKO mice corresponding to images (*D–F*) were stained with Safranin O to reveal cartilaginous matrix (red). In particular, note strong staining of excess bony region around the metaphysis of the metacarpal bone. Note that early stage of disease was developed in the periosteum or perichondrium region (*F, I*). Scale bars = 1 mm (*A, B*), 200 μm (*C, D, E, G, H*), 50 μm (*F, I*).

cartilage. Moreover, we identified the strong staining for FGF2 protein in the SHP2 cKO rib bones (Fig. 6*C*, left two panels) where ectopic cartilage was formed within trabecular bone at random (Fig. 5*E*). FGF2 was also modestly increased in the cKO growth plate (Fig. 6*C*, middle two panels) and was significantly increased in the early stage of ectopic cartilage in the digit (Fig. 6*C*, right panel).

Discussion

The bone phenotype that developed upon induced loss of SHP2 in chondrocytes strongly resembled metachondromatosis in humans. Metachondromatosis contains two pathologic components: one is ectopic cartilage growth toward the outside from the metaphyseal bone called exostosis; another is an ectopic cartilage nodule within the long bones called enchondroma. In the SHP2 cKO mice, an exostosis-like bone phenotype was consistently observed in the metacarpal-phalangeal and metatarsal-phalangeal joints and the distal radius/ulna with continuity from the metaphyseal bone adjacent to the growth plate. A typical enchondroma-like cartilage lesions in the rib bones rather than in the hands and feet was also observed in the SHP2 cKO mice. In metachondromatosis patients, the anatomical site of enchondroma varies considerably between patients in terms of radio-density, size, and location compared with that of exostosis. We believe our SHP2 cKO mouse model is relevant to metachondromatosis found in patients.

The metachondromatosis appeared to develop from the metaphysis of the long bone (Fig. 3*C*). In the cKO mice, we observed an initial formation of ectopic cartilage in the periosteum or perichondrium in the early stage of disease development (Fig. 4*F, I*). The cKO mice also showed a growth plate deformity in the ulna and rib bones (Fig. 5). Therefore, we postulate that the Shp2-deficiency causes two events: 1) growth plate deformity (ie, eutopic event) and 2) extra cartilage formation (ie, ectopic event). We think the former event is not necessary to cause the latter event because early stage of ectopic cartilage was independently observed in the digit where the growth plate is already absent (Fig. 4*F, I*). It is not known whether these two events affect each other at this time.

Cre recombinase was driven by the type II collagen promoter in this study. Therefore, SHP2 should be specifically deleted in cells that express type II collagen (ie, chondrocytes). However, we observed an early stage of disease development in the periosteum or perichondrium (Fig. 4*F, I*), which was positive for X-gal staining (ie, Cre activity) (Supplemental Fig. S2). These findings lead to a possibility that Shp2-deficient chondrocyte progenitor cells in the perichondrium or periosteum caused ectopic cartilage formation, as is reported that the periosteum

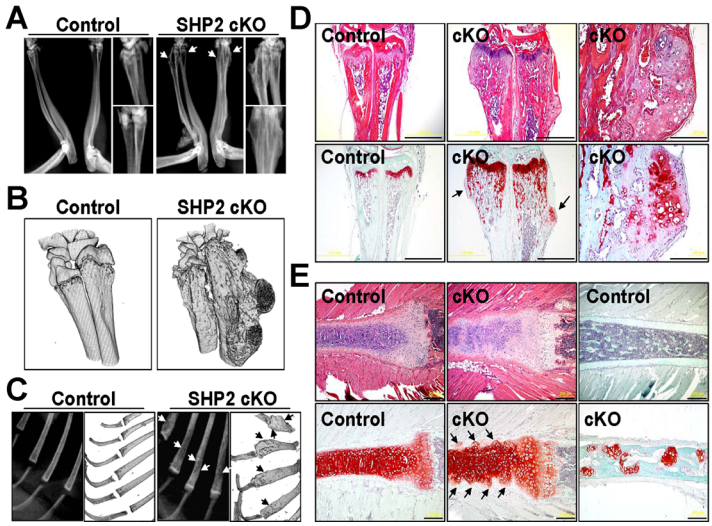

Fig. 5. Radiographic, micro-CT, and histological assessment of forelimbs and ribs of SHP2 cKO mice. (*A*) The forearms from elbow to wrist joints of control and SHP2 cKO mice at 12 weeks of age were assessed by X-ray. Bony exostosis in the distal ulna and radius was identified in the SHP2 cKO mice (arrows). (*B*) The 3D structure of the distal ulna and radius of control and SHP2 cKO mice at 12 weeks of age was assessed by micro-CT using undecalcified samples. The excess bony region was observed in the metaphysis to the diaphysis of the radius and ulna of the SHP2 cKO mouse. (*C*) The ribs of control and SHP2 cKO mice at 12 weeks of age was assessed by X-ray (left) and 3D micro-CT (right). Note irregular rib bone surface and heterogenic radiointensity in the rib bones of the SHP2 cKO mouse (arrows). (*D*) H&E-stained (top row) and Safranin O-stained (bottom row) serial sections of the forearms of control and SHP2 cKO mice at 12 weeks of age. H&E staining showed a bone deformity in the distal radius and ulna of the SHP2 cKO mice with an exostosis-like bony mass compared with the controls. Safranin O staining showed cartilaginous outgrowth in the distal radius and ulna of the SHP2 cKO mouse (arrows). Scale bars = 1 mm. (*E*) H&E-stained (top left two panels) and Safranin O-stained (top right panel and bottom row) serial sections of rib bones of control and SHP2 cKO mice at 12 weeks of age. H&E staining showed a disorganized column formation in the rib growth plate cartilage and an irregular perichondrium/cartilage junction in the SHP2 cKO mice compared with the controls (top two left panels). Safranin O staining showed a disorganized staining pattern in the growth plate and a presence of hypertrophic chondrocyte clusters along the length of the rib cartilage (bottom two left panels). In addition, Safranin O staining showed multiple cartilaginous islands within the rib bones of SHP2 cKO mouse compared with control (top and bottom right panels). Scale bars = 200 μm.

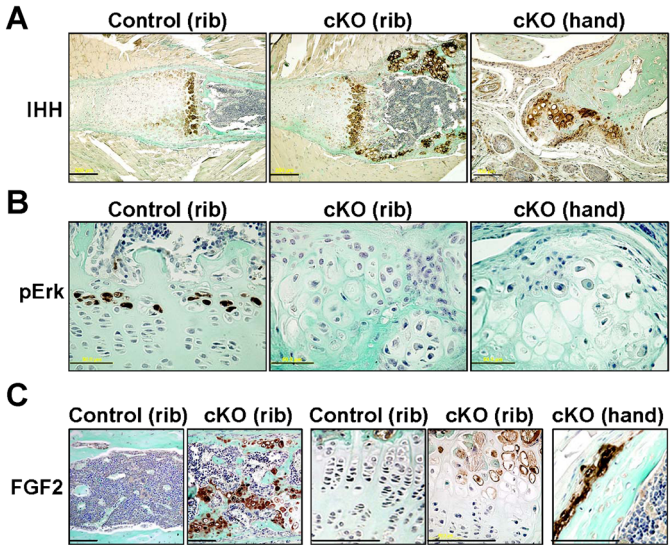

Fig. 6. Impaired MAPK activation and increased expression of IHH in SHP2 cKO mice. (*A*) IHH expression in the SHP2 cKO mice was assessed using an anti-IHH antibody. The region of IHH expression in the rib growth plate cartilage was elongated in SHP2 cKO mice compared with controls and was abundantly expressed in the exostosis-like cartilaginous outgrowth (rib bones, hands) and enchondroma-like cartilaginous islands within bone (rib bones). Scale bars = 200 μm (left, middle), 100 μm (right). (*B*) Amounts of activated Erk MAPK in the SHP2 cKO mice were assessed using an anti-phospho-Erk1/2 antibody. Phospho-Erk staining was readily identified in hypertrophic chondrocytes in the control rib growth plate cartilage but was largely absent from the same cells in SHP2 cKO mice and was undetectable in the cartilaginous nodules of the hand. Scale bars = 50 μm. (*C*) FGF2 protein abundance in SHP2 cKO mice was assessed using an anti-FGF2 antibody. Intense FGF2 protein staining was identified in the trabecular bone area of the ribs in the SHP2 cKO mice, where multiple ectopic cartilage nodules were observed. It was also increased in the cKO rib growth plate compared with control. In the cKO hand, FGF2 was increased in the early stage of disease development. Scale bars = 100 μm.

as well as the perichondrium contains chondrogenic progenitor cells in humans and rodents.[21,22] In terms of efficiency of Cre activity, it is noted that there are X-gal-negative chondrocytes in the cartilaginous nodule lesion (Supplemental Fig. S2). In contrast, both IHH and FGF2 are abundantly expressed within the nodule (Fig. 6). Although the disease mechanism is still unclear at this time, we think there are both cell-autonomous and cell-nonautonomous fashions to develop and progress this disease. This evidence is consistent with the recent interesting finding that only about 6% to 15% of Cre recombination is sufficient for the development of ectopic cartilage formation in the *EXT1* conditional knockout mouse model, suggesting a possibility that inactivation of a target gene in a small fraction of chondrocytes is enough to effect significant phenotypical change by affecting other chondrocytes around the cells initially affected.[19] In addition, when we performed a single tamoxifen injection, we observed the early stage of disease development but not the late stage. Thus, we think multiple tamoxifen injections along with a cell-nonautonomous mechanism may be important for the progression of the disease.

Interestingly, development of the metachondromatosis phenotype in mice may be critically dependent upon the time of SHP2 deletion. In this study, we induced a *Shp2* gene disruption at 4 weeks of age (ie, adolescent stage) and observed a phenotype in autopods (ie, hands and feet) at 6 to 8 weeks, which developed over time up to 12 weeks. However, we did not observe this phenotype when a SHP2 deletion was induced during embryonic stages or in adult mice (ie, 8 weeks) despite that Cre activity was induced at these stages. In addition, we did not see any change of IHH and Erk when we induced a gene disruption at 8 weeks, which may be associated with the absence of the metachondromatosis phenotype. Consistently, in our previous study in which we ubiquitously induced gene disruption at 6 to 8 weeks, we did not observe the metachondromatosis phenotype.[11] Therefore, we believe that SHP2 may have an age-dependent role in cartilage, probably because of the presence of age-dependent cofactor(s) or compensatory mechanism(s). This phenomena of age dependency is consistent with the evidence that metachondromatosis is known as a postnatal pediatric bone disease rather than a congenital or adult disease. Future studies are needed to investigate this interesting finding.

Multiple hereditary exostosis (MHE) has been known as a classic exostosis primarily owing to the gene mutations of EXT1[3] and EXT2[23] that encode a glycosyltransferase essential for heparan sulfate synthesis. MHE-exostoses are usually located in the metaphyseal region of the proximal humerus, distal radius and ulna, proximal tibia, and distal femur, whereas metachondromatosis-exostoses are located in the metaphyseal region of the digit bones (ie, hands and feet). MHE exostoses are normally covered by a well-developed surface cartilaginous cap with endochondral bone formation, whereas metachondromatosis exostoses are covered by a fibrous cap without endochondral bone formation (Fig. 4). It is also known that some MHE patients are negative for genetic tests of EXT1 and EXT2,[24] suggesting an involvement of other unknown molecules as a causative gene of MHE. Similar to our finding, a chondrogenic cell is at least a causative cell type for MHE because a targeted deletion of EXT1 in chondrocytes showed an MHE phenotype in mice.[19] Both metachondromatosis and MHE exhibit ectopic bone growth in metaphyses. It is possible that chondrogenic cells in the periosteum,[22] which surround metaphyseal bone, contribute to the initial outgrowth cartilage formation. As a future direction, it will be interesting to compare the disease mechanisms of exostosis between metachondromatosis and MHE.

Metachondromatosis may be genetically heterogeneous in patients;[1] however, we only observed a metachondromatosis-like phenotype in homozygous SHP2 cKO mice. It is possible that a second hit somatic mutation causes metachondromatosis in humans because SHP2 is known as an important tumor-suppressor gene.[25] It may be a challenge to prove this scenario in patients because of the difficulty of obtaining patient samples. It is of note that germline mutations of the *SHP2* gene in humans may also result in Noonan syndrome (OMIM 163950) and LEOPARD syndrome (OMIM 151100), both of which have skeletal components.[6,7,26,27] However, metachondromatosis is not found in these diseases, suggesting a chondrocyte-specific deficiency of SHP2 is required for the development of this disease.

As a limitation of this study, the cause-consequence of this disease mechanism is still unclear at molecular levels. IHH was abundantly expressed within ectopic cartilage nodules, and this finding is consistent with the current understanding of exostosis or enchondroma where IHH is significantly enhanced.[18,28] However, this could be a consequence of increased population of prehypertrophic chondrocytes. In fact, IHH overexpression in mice using a *Col2a1* promoter did not cause ectopic cartilage.[29] Both the FGF receptor and MAPK that are triggered by FGF are thought to inhibit IHH expression in cartilage.[20,30] In addition, SHP2 is recognized to promote MAPK signaling in other cellular systems.[31] Future studies on IHH, FGF, and MAPK to identify the molecular mechanism responsible for this disease development and progression will be informative.

In conclusion, we have generated a mouse model of metachondromatosis by a targeted disruption of the *Shp2* gene in chondrocytes. In the cartilaginous nodules of exostosis and enchondroma, IHH was abundantly expressed, whereas MAPK signal was reduced. This model will advance the understanding of metachondromatosis and will be used to identify disease cause at molecular levels and to facilitate the development of therapeutic modalities for the treatment of this condition.

Disclosures

All authors state that they have no conflicts of interest.

Acknowledgments

This study was supported by an intramural grant at Texas Scottish Rite Hospital for Children (NK). We thank Ila Oxendine for experimental assays, Tracy Wassell and Amanda McLerran for animal care and surgical assistance, Reuel Cornelia and Richard Banlaygas for histological preparation, and Olumide Aruwajoye for micro-CT scanning.

Authors' roles: DSF, DC, and PDK provided mouse lines. NK designed experiments, reviewed data, and wrote the manuscript. HK and PDK reviewed data and edited the manuscript.

References

1. Bowen ME, Boyden ED, Holm IA, et al. Loss-of-function mutations in PTPN11 cause metachondromatosis, but not Ollier disease or Maffucci syndrome. PLoS Genet. 2011;7(4):e1002050.

2. Sobreira NL, Cirulli ET, Avramopoulos D, et al. Whole-genome sequencing of a single proband together with linkage analysis identifies a Mendelian disease gene. PLoS Genet. 2010;6(6): e1000991.
3. Ahn J, Ludecke HJ, Lindow S, et al. Cloning of the putative tumour suppressor gene for hereditary multiple exostoses (EXT1). Nat Genet. 1995;11(2):137–43.
4. Kennedy LA. Metachondromatosis. Radiology. 1983;148(1):117–8.
5. Dechert U, Duncan AM, Bastien L, Duff C, Adam M, Jirik FR. Protein-tyrosine phosphatase SH-PTP2 (PTPN11) is localized to 12q24.1-24.3. Hum Genet. 1995;96(5):609–15.
6. Tidyman WE, Rauen KA. The RASopathies: developmental syndromes of Ras/MAPK pathway dysregulation. Curr Opin Genet Dev. 2009;19(3):230–6.
7. Aoki Y, Niihori T, Narumi Y, Kure S, Matsubara Y. The RAS/MAPK syndromes: novel roles of the RAS pathway in human genetic disorders. Hum Mutat. 2008;29(8):992–1006.
8. Ahmad S, Banville D, Zhao Z, Fischer EH, Shen SH. A widely expressed human protein-tyrosine phosphatase containing src homology 2 domains. Proc Natl Acad Sci USA. 1993;90(6):2197–201.
9. Qu CK, Yu WM, Azzarelli B, Cooper S, Broxmeyer HE, Feng GS. Biased suppression of hematopoiesis and multiple developmental defects in chimeric mice containing Shp-2 mutant cells. Mol Cell Biol. 1998; 18(10):6075–82.
10. Saxton TM, Henkemeyer M, Gasca S, et al. Abnormal mesoderm patterning in mouse embryos mutant for the SH2 tyrosine phosphatase Shp-2. EMBO.J. 1997;16(9):2352–64.
11. Bauler TJ, Kamiya N, Lapinski PE, et al. Development of severe skeletal defects in induced SHP-2-deficient adult mice: a model of skeletal malformation in humans with SHP-2 mutations. Dis Model Mech. 2011;4(2):228–39.
12. Chen M, Lichtler AC, Sheu TJ, et al. Generation of a transgenic mouse model with chondrocyte-specific and tamoxifen-inducible expression of Cre recombinase. Genesis. 2007;45(1):44–50.
13. Soriano P. Generalized lacZ expression with the ROSA26 Cre reporter strain. Nat Genet. 1999;21(1):70–1.
14. Livak KJ, Schmittgen TD. Analysis of relative gene expression data using real-time quantitative PCR and the 2(-Delta Delta C(T)) Method. Methods. 2001;25(4):402–8.
15. Kamiya N, Ye L, Kobayashi T, et al. Disruption of BMP signaling in osteoblasts through type IA receptor (BMPRIA) increases bone mass. J Bone Miner Res. 2008;23(12):2007–17.
16. Kamiya N, Kobayashi T, Mochida Y, et al. Wnt inhibitors Dkk1 and Sost are downstream targets of BMP signaling through the type IA receptor (BMPRIA) in osteoblasts. J Bone Miner Res. 2010;25(2): 200–10.
17. Kamiya N, Ye L, Kobayashi T, et al. BMP signaling negatively regulates bone mass through sclerostin by inhibiting the canonical Wnt pathway. Development. 2008;135(22):3801–11.
18. Bovee JV, Hogendoorn PC, Wunder JS, Alman BA. Cartilage tumours and bone development: molecular pathology and possible therapeutic targets. Nat Rev Cancer. 2010;10(7):481–8.
19. Matsumoto K, Irie F, Mackem S, Yamaguchi Y. A mouse model of chondrocyte-specific somatic mutation reveals a role for Ext1 loss of heterozygosity in multiple hereditary exostoses. Proc Natl Acad Sci USA. 2010;107(24):10932–7.
20. Kronenberg HM. Developmental regulation of the growth plate. Nature. 2003;423(6937):332–6.
21. De Bari C, Dell'Accio F, Luyten FP. Human periosteum-derived cells maintain phenotypic stability and chondrogenic potential throughout expansion regardless of donor age. Arthritis Rheum. 2001; 44(1):85–95.
22. Ito Y, Fitzsimmons JS, Sanyal A, Mello MA, Mukherjee N, O'Driscoll SW. Localization of chondrocyte precursors in periosteum. Osteoarthritis Cartilage. 2001;9(3):215–23.
23. Stickens D, Clines G, Burbee D, et al. The EXT2 multiple exostoses gene defines a family of putative tumour suppressor genes. Nat Genet. 1996;14(1):25–32.
24. Wuyts W, Van Hul W. Molecular basis of multiple exostoses: mutations in the EXT1 and EXT2 genes. Hum Mutat. 2000;15(3): 220–7.
25. Mohi MG, Neel BG. The role of Shp2 (PTPN11) in cancer. Curr Opin Genet Dev. 2007;17(1):23–30.
26. Conti E, Dottorini T, Sarkozy A, et al. A novel PTPN11 mutation in LEOPARD syndrome. Hum Mutat. 2003;21(6):654.
27. Tartaglia M, Gelb BD. Noonan syndrome and related disorders: genetics and pathogenesis. Annu Rev Genomics Hum Genet. 2005;6:45–468.
28. Hopyan S, Gokgoz N, Poon R, et al. A mutant PTH/PTHrP type I receptor in enchondromatosis. Nat Genet. 2002;30(3):306–10.
29. Long F, Zhang XM, Karp S, Yang Y, McMahon AP. Genetic manipulation of hedgehog signaling in the endochondral skeleton reveals a direct role in the regulation of chondrocyte proliferation. Development. 2001;128(24):5099–108.
30. Minina E, Kreschel C, Naski MC, Ornitz DM, Vortkamp A. Interaction of FGF, Ihh/Pthlh, and BMP signaling integrates chondrocyte proliferation and hypertrophic differentiation. Dev Cell. 2002;3(3): 439–49.
31. Dance M, Montagner A, Salles JP, Yart A, Raynal P. The molecular functions of Shp2 in the Ras/Mitogen-activated protein kinase (ERK1/2) pathway. Cell Signal. 2008;20(3):453–9.